ISBN: 978-3-95450-240-0 ISSN: 2673-5539 doi:10.18429/JACoW-RuPAC2021-WEPSC16

NUMERICAL RESEARCH OF DESIGN SOLUTIONS FOR THE BENDING MAGNETS OF THE ELECTRON BEAM FACILITY GESA-1M

N. Kazachenko†, E. Gapionok, V. Kukhtin, I. Rodin, K. Tkachenko,
JSC "NIIEFA", St. Petersburg, Russia
D. Ovsyannikov, S. Sytchevsky, St.Petersburg State University, Russia

Abstract

Comparative simulations of magnet configurations have been performed searching for the optimum design of bending magnets for the intense pulsed electron beam facility GESA-1M. The beam trajectory through electric and magnetic fields was simulated for three candidate configurations of the bending magnets. A comparison was focused on the expected power density and divergence angle at the target. The most efficient concept was found to be two pairs of coils arranged orthogonally to each other. This configuration produces highly uniform distribution of the current density at the target, the divergence angle being as low as several degrees. An important advantage is that the initial beam power can be intensified by a 20% at the target.

INTRODUCTION

GESA-1M is used for improvement of material surface properties and is capable to generate a 120 kV, 10 A/cm^2, 50 µs electron beam with the diameter of 10 cm. One of specific concerns is to prevent the beam path from micro-contaminations from the irradiated surface. To overcome this problem a system of bending magnets is used to guide and deflect particles. The best efficiency is observed when the electron beam is deposited normally to the surface, and a constant power density is kept across the beam spot. The study has been carried out for three candidate design options illustrated in Fig. 1.

COMPUTATIONAL PROCEDURE

All electrons in a pulse were assumed to have the same energy of 120 keV. Each electron trajectory was taken tangentially to a field line at the starting point. The starting points were taken on a horizontal plane on the upper surface of the top coil at $Z = 42$ cm. The vertical electron momentum is directed opposite to the axis Z.

An electron moves according to the Newtonian equations of motion. Using the Gaussian system of units, the electron motion can be represented in a vector form as

$$\begin{cases} d\vec{p'}/ds = \vec{E'}/\beta + [\vec{\beta}, \vec{H'}]/\beta \\ d\vec{r}/ds = \vec{p}'/p' \end{cases}$$

Here $\vec{p} = \vec{\beta}/\sqrt{1-\beta^2}$ is the relativistic momentum, $\vec{\beta}$ is the electron velocity, s is the trajectory length, $\vec{r}$ is the position vector, $\vec{E}' = e\vec{E}/E_0$ and $\vec{H}' = e\vec{H}/E_0$ are respective vectors of relative electric and magnetic field strength, e is the electron charge, E_0 is the self-energy.

† kazachenko-sci@yandex.ru

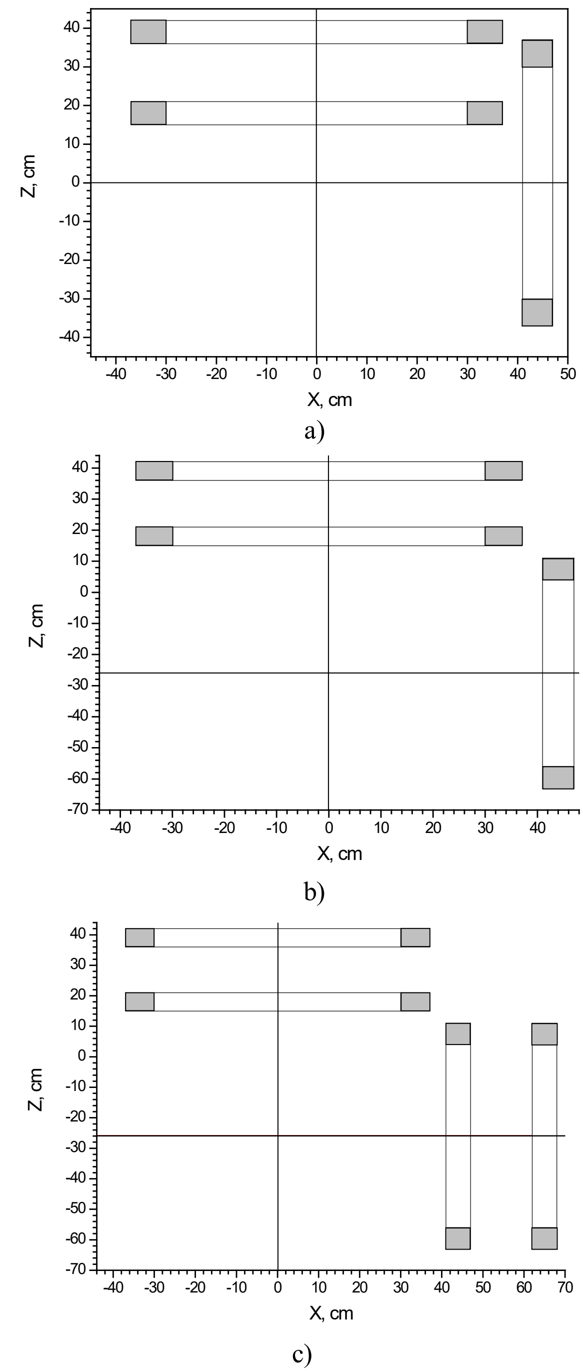

Figure 1: Bending magnet. a) Design option #1, b) Design option #2, c) Design option #3.

A space charge electric field was taken zero assuming magnetic field of the bending magnet is high enough to

ISBN: 978-3-95450-240-0 ISSN: 2673-5539 doi:10.18429/JACoW-RuPAC2021-WEPSC16

neglect space-charge repulsion. The total momentum p' was assumed constant.

The starting points were taken on concentric circles with the radius R_0 varying in the range from 0 to 5 cm. The point coordinates were determined as in the $x_0 = R_0 \cdot \cos\varphi$, $y_0 = R_0 \cdot \sin\varphi$, $z_0 = 42$ cm, where φ is the angle between the position vector of a starting point and axis X ranging from 0 to 2π. Components of the total momentum at every starting point were determined as $p'_{x0} = -p' \cdot \left(\frac{H_x}{H}\right)$, $p'_{y0} = -p' \cdot \left(\frac{H_y}{H}\right)$, $p'_{z0} = -p' \cdot \left(\frac{H_z}{H}\right)$, where H_x, H_y, H_z, H were observed at the origin of coordinates (x_0, y_0, z_0). The electron trajectory was derived by solving the above system of equations using Adams' method [1,2]. Field strength components H_x, H_y, H_z were evaluated in simulations with electromagnetic code KLONDIKE [3, 4].

The every trajectory was ended at the target surface. At the end point components of the total momentum of an electron and its incident angle were calculated. The target surface was located normally to the axis X at a 1 cm distance away from the vertical coil at the exit of the bending magnet (see Fig. 1). The beam energy density was evaluated over 4 trajectories started from the vertices of a small quadrangle on the $Z = 42$ cm plane. The quadrangle area was pre-determined in test simulations. The starting quadrangle was projected on the target surface with controllable curvature. Observation points were taken over the projection. The energy density on the irradiated surface was evaluated via the ratio of the starting and projected areas.

RESULTS OF TRAJECTORY SIMULATIONS

Plots on Figs. 2, 3, 4 present incident angles calculated for 3 design options of the bending magnet. Option #1 demonstrates the most non-uniform angular distribution. The highest deflection is detected near the beam periphery reaching 13°. The incident angle above the admissible value of 10° occurs for almost a half of electrons. Asymmetry of the angular distribution is resulted from the electron drift due to the field inhomogeneity. Option #2 provides the incident angles below 7°. For Option #3 the incident angle as low as 4° is observed over the entire irradiated surface. Weak asymmetry of the angular distribution occurs with respect to the plane Y = 0.

Figs. 5, 6, 7 illustrate simulated current density over the target. Again, Option #1 demonstrates the most non-uniform distribution of the current density. Options #2, #3 provide good uniformity of the current density distribution. A 30% reduction of the current density on the target surface as compared to the emitted beam is observed for Option #2. This means that the beam spot on the target is larger than the aperture. For Option 3 the current density remains unchanged.

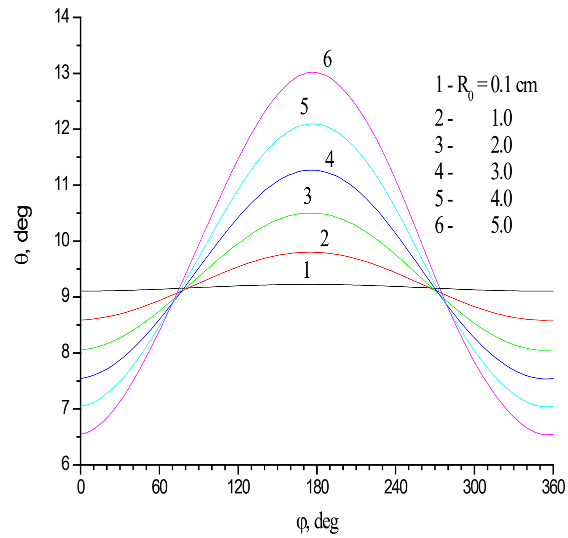

Figure 2: Incident angle θ vs. polar angle φ, for various trajectories. Design option #1.

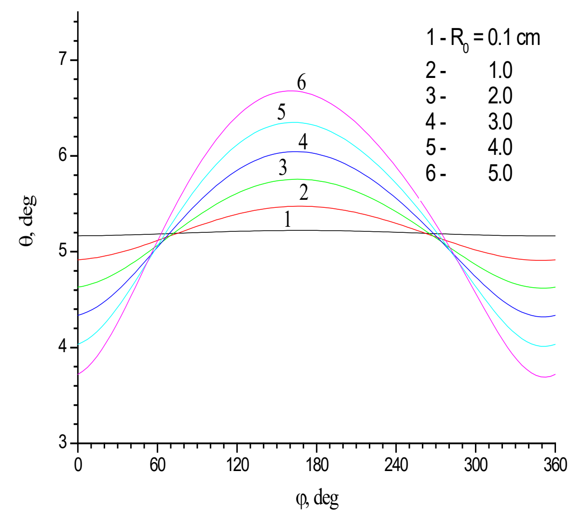

Figure 3: Incident angle θ vs. polar angle φ, for various trajectories. Design option #2.

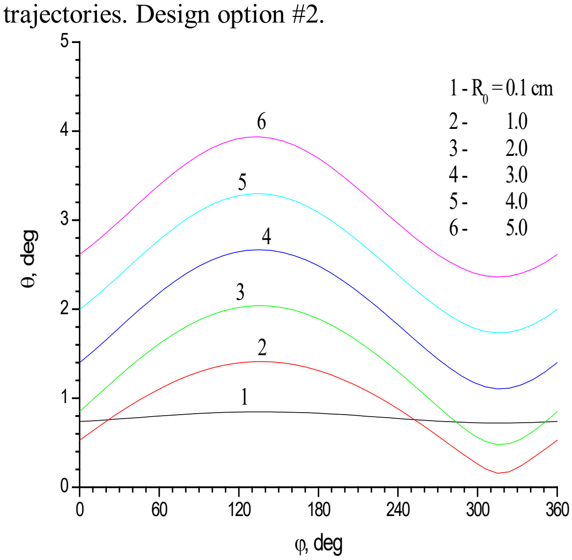

Figure 4: Incident angle θ vs. polar angle φ, for various trajectories. Design option #3.

ISBN: 978-3-95450-240-0 ISSN: 2673-5539 doi:10.18429/JACoW-RuPAC2021-WEPSC16

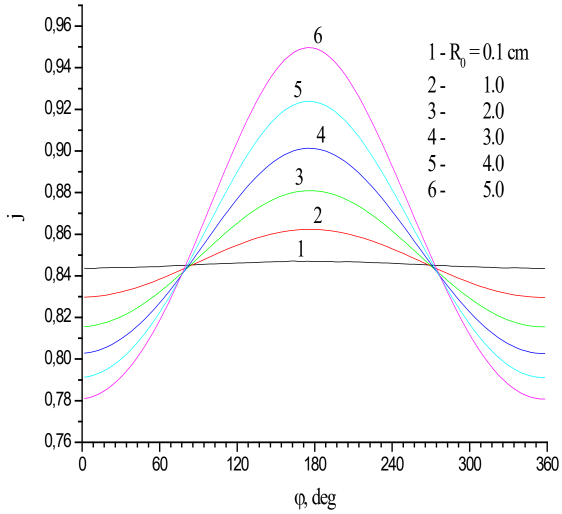

Figure 5: Current density on target surface for various trajectories. Design option #1.

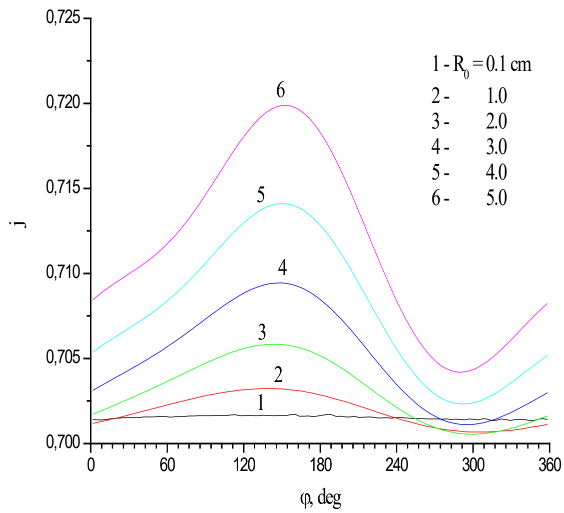

Figure 6: Current density on target surface for various trajectories. Design option #2.

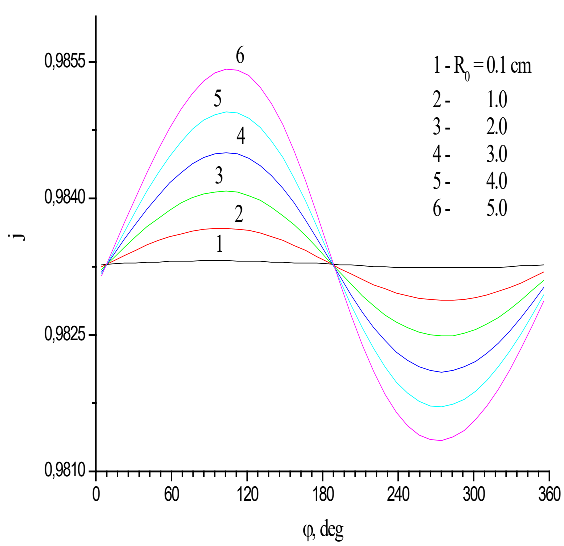

Figure 7: Current density on target surface for various trajectories. Design option #3.

CONCLUSIONS

The most efficient concept was found to be configuration #3 with two pairs of coils arranged orthogonally to each other. Such bending magnet provides highly uniform distribution of the current density at the target with the incident angle as low as 4º.

These evaluations have been obtained assuming the initial electron velocity at the starting point is co-directed with the field line. Also, space-charge repulsion was neglected. A further study is necessary to assess the error introduced with these assumptions.

REFERENCES

[1] N.Kalitkin. Numerical methods (in Russian), Moscow, Nauka Publ., 1978.

[2] O.Arushunyan, S.Zalyotkin. Numerically solving ordinary differential equation in FORTRAN (in Russian), Moscow, Moscow State University Publ., 1990.

[3] V. Amoskov *et al.*, "Computation technology based on KOMPOT and KLONDIKE codes for magnetostatic simulations in tokamaks", *Plasma Devices Oper.*, vol. 16, no.2, pp.89-103, 2008, doi:10.1080/10519990802018023

[4] V.M. Amoskov *et al.*, "Magnetic model MMTC-2.2 of ITER tokamak complex", *Vestnik of Saint Petersburg University, Applied Mathematics. Computer Science. Control Processes*, vol. 15, no. 1, pp. 5-21, 2019, doi: 10.21638/11702/spbu10.2019.101